1999

# On the efficiency of stereologic volumetry as commonly implemented for 3D digital images

Kevin J. Black
*Washington University School of Medicine in St. Louis*

**On the efficiency of stereologic volumetry as commonly implemented for 3D digital images**

(REVISED VERSION December 7, 1998)

Kevin J. Black, M.D.

Departments of Psychiatry and of Neurology and Neurological Surgery, and Mallinckrodt Institute of Radiology, Washington University School of Medicine, St. Louis, MO

Short title: **efficiency of 3D stereologic volumetry**

Campus Box 8225

4525 Scott Ave.

St. Louis, MO 63110

Phone 314-362-6908

FAX 314-362-0168

e-mail kevin@npg.wustl.edu

# On the efficiency of stereologic volumetry as commonly implemented for 3D digital images

Short title: **efficiency of 3D stereologic volumetry**

**ABSTRACT:**

*Purpose:* To demonstrate, for certain ideal shapes (right cylinders) and for representative neuroanatomical images, that stereologic volumetry of 3D images is more efficient when the sampling grid is placed randomly on each cross-section rather than identically across sections.

*Materials and Methods:* Right cylinders: mathematical proof. Neuroanatomical images: a custom computer program estimated volume with either the fixed- or random-grid method, using the same cross-sectional slices and first-slice test grid position for each method. The slice spacing, grid size, and starting grid position were randomly varied within practical constraints for 100,000 trials in each image.

*Results:* For right cylinders, the random-grid method is always more efficient than the fixed-grid method. For the neuroanatomic images tested, relative variance was up to three times higher for the fixed-grid method than for the random-grid method, especially for test grids with few grid intersections ("hits") per section. With the random-grid method, relative variance is primarily dependent on the total number of hits rather than on the distribution of hits per section.

*Conclusion:* Implementation of the random-grid method for stereologic volumetry in 3D images should in general improve sampling efficiency.

**MeSH key words:**

image processing, computer-assisted

stereology

volumetry

methods

**Introduction:**

Several important biological questions can be expressed in terms of a measurement of volume, and important biological results have come from volume measurements of all or parts of various organs (*e.g.*, (Jack et al. 1992; Sheline et al. 1996b; Krishnan and Doraiswamy 1997; Nemeroff et al. 1992; Oster et al. 1993; Garden and Roberts 1996) ). Although originally the domain of pathologists and anatomists, volumetric measurements are now also applied to medical images.

Stereology provides a mathematically sound method of measuring volume, and tutorial reviews of its application to neuroimaging are available (Mayhew and Olsen 1991; Gundersen 1992; Krishnan et al. 1993) . Commonly it is implemented as a two-stage procedure in which finding the volume of an object is first reduced to area measurements of properly chosen parallel cross sections. Area measurements of the cross sections are then found by applying a regular square lattice of test points and counting the intersections of the grid points with the object of interest.

Stereology has several advantages. First, this technique provides unbiased volume measurement even for irregularly shaped structures. Stereology also allows valid 3D measurements from 2D images, which was crucial before the development of current 3D structural imaging techniques (MacFall et al. 1994). A third key advantage of stereologic volumetry, and the one addressed in this report, is its superior efficiency when compared to older methods. That is, for the same number of data points sampled, the variance of the stereologic volume measurement is substantially lower. Quantitative estimates of this improvement in

variance can be derived from the mathematical theory (Gundersen and Jensen 1987) , and in practice, stereology can save time over other volumetric methods (Keshavan et al. 1995) .

However, in volumetric studies with my colleagues using 3D digital images, it appeared that the actual measured efficiency was not as high as we had estimated using these assumptions (Haller et al. 1994; Sheline et al. 1995; Sheline et al. 1996a; Black et al. 1998) . It seemed reasonable that this discrepancy might be due to specific details of the implementation of stereologic volumetry for 3D discrete images. The most obvious such detail is the fact that in the case of 3D digital images, successive 2D slices are aligned along a common $z$ axis rather than at random. Several commonly used computer programs that implement stereologic volumetry for 3D images allow random positioning of the test grid on the first cross-section but then superimpose the grid at the same, fixed, location on each subsequent section, contrary to the random-placement assumption of the original method. This derives from a general belief that the two methods are essentially equivalent (e.g., (Roberts 1993) ). Unfortunately, quantitative predictions of the efficiency of stereologic volumetry rely on an assumption that the test grid be applied "at random" to each section (Gundersen et al. 1988 p. 383), a requirement easily satisfied for histologic sections or other 2D images but violated by the commonly-used implementations described above.

Fortunately it can be shown that this 3D "fixed-grid" technique still provides an unbiased (accurate) estimator of volume. However, in this report I provide evidence that this is less efficient than applying the test grid at random on successive slices. I first prove that the fixed-grid technique is less efficient for the special case of certain ideal structures, *i.e.* cylinders, and then show that it is also less efficient for measuring a variety of relevant neuroanatomical images.

**Materials and Methods:**

*Special case.* For the special case of mathematical right cylinders (*i.e.* images in which the cross-section on each slice is identical), an example is given in Figure 1 and an informal proof is presented in Results.

*Images.* Images representing solid cubes and circular cylinders were created using ANALYZE v. 7.5 (Mayo Biomedical Imaging Resource, Rochester, MN) (Robb and Barillot 1989) . Neuroanatomical images were derived from previous studies (Haller et al. 1994; Black et al. 1997; Black et al. 1998) , and were edited using ANALYZE so that the structure of interest represented the only nonzero voxels in the image.

*Volumetry.* A custom computer program ("stereo", available at http://www.imaging.wustl.edu/kevin/stereo.htm) was written in the C programming language and implemented on a Sparc10 running SunOS 4.1.3 (Sun Microsystems, Inc., Palo Alto, CA). The program measures the volume of all nonzero voxels in two ways: "fixed-grid" and "random-grid," as follows. Assume the voxels in a 3D image with dimensions $xdim \times ydim \times zdim$ are indexed as $(i, j, k)$. For a given distance $\Delta z$ between sampled slices, and a given square grid spacing $\Delta x \times \Delta x$, a random start position $(i_0, j_0, k_0)$ is chosen with $i_0, j_0 \in (1, ..., \Delta x)$, $k_0 \in (1, ..., \Delta z)$. For each method, the volume in voxels is estimated as $V_{est.} = \Delta z \cdot (\Delta x)^2 \cdot \Sigma p_k$ , where $p_k$ is the number of nonzero intersections of the sampling grid with the image on slice $k$, and the summation is taken over all $k \in (1, ..., zdim)$ satisfying $k \equiv k_0 \pmod{\Delta z}$. For the fixed-grid method, the grid is at the same location on each slice, whereas for the random-grid method, the position of the grid on each slice is random.

For each combination of image, image orientation, slice spacing, and grid size, the program estimates volume using both the fixed-grid and random-grid methods. This procedure was repeated 100,000 times; for any given trial, the same start slice and first-slice grid position were used for both fixed- and random-grid measurements. Then for each image and image orientation, this process was repeated for all possible combinations of slice spacing and grid size which satisfied the following criteria: $\Delta x$ and $\Delta z$ were between 2 and 20, the mean number of slices intersecting the object was more than 3.5, and the mean number of "hits," $\Sigma p_k$ , was between 35 and 300.

*Statistics.* With an N of 100,000, the *F*-statistic used to compare variances of two different measurements is significant at any variance ratio other than 1.000. Thus for each combination of image, image orientation, slice spacing, and grid size, we can definitively state that the variance of the volume estimates is greater either for the fixed-grid or the random-grid method. Since there were many such combinations possible for each image (see Table 1, column 2), I report the probability (from the binomial distribution) that the observed distribution of "wins" for either method could happen by chance, if the probability of one method "winning" for any given combination were 50%. Since there was a directional hypothesis, one-tailed *p* values are reported.

For ease of comparison between images with different volumes, the coefficient of variation (CV = √variance / mean) is reported. Since the mean volumes using either method were essentially identical, this does not affect the results.

*Exploration of factors influencing $CV_{random}$.* For exploring test grid contributions to relative variance with the random-grid method, I fit a least-squares line using (average total

number of hits)$^{-1/2}$ as the independent variable and $CV_{random}$ as the dependent variable, across all test grids used for each image and orientation. The strength of this correlation is reported using Pearson's *r*. The residuals after fitting this line (that is, actual CV minus predicted CV) were then graphed as a function of the ratio of total hits to the number of slices with nonzero intersections.

**Results:**

*Special case.*

Here I provide proof that when measuring certain solids, including right cylinders, the fixed-grid method always has a variance higher than or equal to that of the random-grid method (see Figure 1).

Consider any finite, discrete 3D image $(1, \ldots, m)^3 \rightarrow \square$, indexed as $(i, j, k)$ and described with $x$, $y$, and $z$ axes, and any set of points S in that image which satisfies the following criterion. Any nonempty intersection of S with any $xy$ image plane is identical. In other words, if a point $(i_0, j_0, k_0)$ is in S and the plane $z = k_1$ intersects S, then $(i_0, j_0, k_1)$ is also in S.

Now estimate the volume of S using the "fixed-grid" and the "random-grid" stereologic methods described above, for a given selection of equidistant cross-sections, $n$ of which intersect S non-trivially. If $\Delta z$ is the slice spacing and $A_1 \ldots A_n$ are the number of test grid intersections on each of the nonzero cross-sections, then the two estimates of S's volume are: $V_{\text{fixed}} = \Delta z \cdot \Sigma A_i = \Delta z \cdot \Sigma A_1 = \Delta z \cdot n \cdot A_1$ (since the test grid and cross-section are identical on each slice), and $V_{\text{random}} = \Delta z \cdot \Sigma A_i$ (which in general $\neq \Delta z \cdot n \cdot A_1$, since the test grid placement can vary from slice to slice).

For either technique, because of the criterion above describing S, the variances of each

area measurement across all possible test grid placements satisfy $\mathrm{var}(A_1) = \ldots = \mathrm{var}(A_n)$. Also recall that for random variables $x_i$, $\mathrm{var}(x_1 + \ldots + x_n) = \Sigma_i \Sigma_j \mathrm{cov}(x_i, x_j)$, where $\mathrm{cov}(x_i, x_i) = \mathrm{var}(x_i)$. Combining these facts with the volume estimates from the preceding paragraph, we obtain $\mathrm{var}(V_{\mathrm{random}}) = (\Delta z)^2 \cdot \Sigma_i \Sigma_j \ \mathrm{cov}(A_i, A_j)$, and $\mathrm{var}(V_{\mathrm{fixed}}) = (\Delta z)^2 \cdot n^2 \cdot \mathrm{var}(A_1)$.

An intuitive way of comparing these is by rewriting the covariates using the Pearson correlation coefficients $r_{i,j}$ which describe the correlation between the area estimates $A_i$ on different slices. Since all the slice variances are equal, $r_{i,j} = \mathrm{cov}(A_i, A_j)/\mathrm{var}(A_1)$. Solving this for the covariance and substituting, we obtain $\mathrm{var}(V_{\mathrm{random}}) = (\Delta z)^2 \cdot \Sigma_i \Sigma_j \ r_{i,j} \cdot \mathrm{var}(A_1)$. From this equation we can see that the variance of the stereologic volume estimate depends on the correlation between area estimates on different slices. Since slice areas are perfectly correlated for fixed-grid measurements of S ($r_{i,j} = 1$ for all $i$ and $j$), this gives the highest possible variance, $\mathrm{var}(V_{\mathrm{fixed}}) = (\Delta z)^2 \cdot n^2 \cdot \mathrm{var}(A_1)$. For the random-grid case, the correlation between slice area estimates will be in general less than 1 so that $\Sigma_i \Sigma_j \ r_{i,j} \leq n^2$, implying that $\mathrm{var}(V_{\mathrm{random}}) \leq \mathrm{var}(V_{\mathrm{fixed}})$ (QED). For instance, in the unlikely special case that area estimates on different slices are completely independent of each other (zero correlation for $i \neq j$), then $\mathrm{var}(V_{\mathrm{random}}) = (\Delta z)^2 \cdot \ n \cdot \ \mathrm{var}(A_1) = (1/n) \cdot \mathrm{var}(V_{\mathrm{fixed}})$.

*Simulations using geometric and neuroanatomical test images.*

Compared to the actual volume by exhaustive voxel count, mean volumes after 100,000 trials were always accurate to within 0.1% using either method.

For the cylindrical test images there were 117 different image - test grid combinations which met the stated criteria. The relative variance, CV, was never less for volume estimates

using the fixed-grid method than for comparable estimates using the same slice distance but using the random-grid method (see Table 1). The median ratio of relative variances was $CV_{fixed}/CV_{random} = 1.993$, and for some image - test grid combinations this ratio was as high as 3.470.

For the cube measured 45° to any edge, the two methods were similar; only about half the possible slice - grid combinations gave $CV_{fixed} > CV_{random}$ (see Table 1).

To show that 100,000 measurement trials were sufficient to reproducibly estimate the relative variance in the volume measurements, I repeated the procedure for these images and compared the CV estimates from the first and second groups of 100,000 trials. There was near-perfect correspondence ($r > 0.9999$).

For the various neuroanatomical images tested, there were certain combinations of image, image orientation, slice distance, and grid spacing for which $CV_{fixed}$ was slightly smaller than $CV_{random}$. In general the two methods were quite similar, so that when averaged across all grids, the difference in CV was modest, in the most extreme case 6.5% vs 4.6%. Even then, for most images tested, the random-grid method was more efficient overall (see Table 1).

However, for many individual grids the CV was 2 to 3 times higher with the fixed method than with the random method. The converse was not true, as $CV_{fixed}$ was never less than ¾ of $CV_{random}$. After comparing a number of parameters across these images, it appeared that one feature of the sampling grid could predict when the fixed-grid variance was likely to differ substantially. This feature was the average number of hits on cross sections which intersected the image. As shown in Figure 2, when the average number of hits on each slice was high (10-30 or more), the relative variance was similar with either method, but for lower values of this

parameter there were many sampling grids for which the random-grid method was markedly superior.

As these results demonstrate the superiority of the random-grid method, I explored what factors lead to higher or lower variance when applying the random-grid method to real neuroanatomical images. As expected, the relative variance is strongly predicted by the total number $n$ of hits, decreasing as $1/\sqrt{n}$ (see Table 2). However, after accounting for this effect, there was little additional variance added by changes in the average number of hits on each slice intersecting the object (see Table 2 and Figure 3).

**Discussion:**

These results demonstrate that the efficiency of stereologic volumetry for 3D images depends on the details of its implementation. When the 2D sampling grid is placed at a fixed location across all slices sampled, variance can be much higher than when the grid position is random for each slice. The magnitude of this effect depends on which image is being measured (it is worst for cylinder-like objects; see Table 1) and on the test grid (it is worst for grids which produce fewer average intersections per slice; see Figure 2).

The error in stereologic volumetry has two components, corresponding to the two stages of measurement: error resulting from estimating volume using selected cross-sectional areas, and error from estimating area on the cross-sections using a 2D sampling grid. In this study the sections used in each individual trial were identical for the fixed-grid and random-grid methods, so any differences in variance are attributable only to the second component. This helps explain the generally small average differences between methods for most of the anatomic images tested.

One might also conclude from this fact that increasing the number of slices for a given number of grid points intersecting the object would reduce overall variance, since this would diminish the contribution of the sampling grid placement to overall error (Gundersen and Jensen 1987; Pache et al. 1993) . However, as shown in Figure 2, the opposite was the case; when a large number of test points intersected the object on each slice, the 3D arrangement of the test points was less relevant, presumably since the area measurements were more precise.

These results suggest several practical considerations for investigators designing a new stereological volumetry study for objects in 3D images. First, the random-grid rather than the fixed-grid method should be implemented and used. Avoiding fixed-grid implementations is especially important if the object and test grid used result in less than about 20 “hits” on an average nonempty cross-section. Second, investigators have some guidelines as to how to define the test grid. When using the random-grid method, the results of Gundersen and Jensen (1987) apply. They show that by first measuring certain shape characteristics of the object in question, one can then use stereological theory to estimate the number of sections and total number of hits required for a given degree of accuracy (Gundersen and Jensen 1987 [see p. 249]; Gundersen 1992; Gundersen 1992; 1992) . Alternatively, investigators with access to a SunOS workstation may further test the characteristics of several different grid sizes by segmenting one representative object, running the “stereo” program described in Methods, and choosing a grid size favorable to that sample image. However, in a practical sense, the results shown in Table 2 and Figure 3 suggest that for several neuroanatomical objects, the main determinant of accuracy when using the random grid method is the total number of hits. After accounting for the total number of hits, increasing grid density versus number of slices has little meaningful effect on

variance except at extreme values.

One technical point that should be mentioned is that in this study the sampling grid was always placed orthogonally to the image planes. In general, randomization of the angular orientation of the test grid to the cross-sectional planes may further reduce error, and is a premise of the commonly used formula for quantitative estimation of sampling error in stereologic volumetry (Gundersen and Jensen 1987) . However, this difference does not compromise the present study since the random-grid method clearly outperformed the fixed-grid method for the circular cylinders, and the angular orientation of the grid is irrelevant in these radially symmetric objects.

In summary, implementation of the random-grid method for stereologic volumetry in 3D images will in general improve sampling efficiency, especially for certain shapes and test grids.

**Acknowledgments:**

Thanks to Tom O. Videen, Ph.D., for his patient answers to my C programming questions, to Tamara Hershey, Ph.D., for her patient answers to my statistical questions, to John W. Haller, Ph.D., for the hippocampal image, to an anonymous reviewer, and to Yvette I. Sheline, M.D., and Joel S. Perlmutter, M.D., for research mentorship. Supported by NIH grant NS-01898; a Young Investigator award from NARSAD; the American Parkinson Disease Association; the Charles A. Dana Foundation (The Dana Clinical Hypotheses Research Program); and the McDonnell Center for Higher Brain Function.

**References**

Black, K.J., Gado, M.H., Videen, T.O., Perlmutter, J.S., 1997. Baboon basal ganglia stereotaxy using internal MRI landmarks: validation and application to PET imaging. Journal of Computer Assisted Tomography 21, 881-886.

Black, K.J., Öngür, D., Perlmutter, J.S., 1998. Increased putamen volume in idiopathic focal dystonia. Neurology 51, 819-824.

Garden, A.S., Roberts, N., 1996. Fetal and fetal organ volume estimations with magnetic resonance imaging. Am J Obstet Gynecol 175, 442-448.

Gundersen, H.J.G., 1992. Stereology: the fast lane between neuroanatomy and brain function -- or still only a tightrope? Acta Neurologica Scandinavica Supplementum 137, 8-13.

Gundersen, H.J.G., Bendtsen, T.F., Korbo, L., Marcussen, N., Møller, A., Nielsen, K., Nyengaard, J.R., Pakkenberg, B., Sørensen, F.B., Vesterby, A., West, M.J., 1988. Some new, simple and efficient stereological methods and their use in pathological research and diagnosis. Acta Pathologica, Microbiologica et Immunologica Scandinavica 96, 379-394.

Gundersen, H.J.G., Jensen, E.B., 1987. The efficiency of systematic sampling in stereology and its prediction. Journal of Microscopy 147, 229-263.

Haller, J.W., Botteron, K.N., Brunsden, B.S., Sheline, Y.I., Walkup, R., Black, K.J., Gado, M.H., Vannier, M.W., 1994. Hippocampal MR volumetry. In: Robb, R.A. (Ed.), Visualization in Biomedical Computing 1994 (SPIE Proceedings vol. 2359). pp. 660-671.

Jack, C.R., Sharbrough, F.W., Cascino, G.D., Hirschorn, K.A., O'Brien, P.C., Marsh, W.R., 1992. Magnetic resonance image-based hippocampal volumetry: correlation with outcome after temporal lobectomy. Annals of Neurology 31, 138-146.

Keshavan, M.S., Anderson, S., Beckwith, C., Nash, K., Pettegrew, J.W., Krishnan, K.R.R., 1995. A comparison of stereology and segmentation techniques for volumetric measurements of lateral ventricles in magnetic resonance imaging. Psychiatry Research: Neuroimaging 61, 53-60.

Krishnan, K.R.R., Boyko, O.B., McDonald, W.M., Charles, H.C., MacFall, J.R., Tupler, L.A., Upchurch, L., 1993. Magnetic resonance morphometry: image analysis methodology development for affective disorder. Depression 1, 159-179.

Krishnan, K.R.R., Doraiswamy, P.M., 1997. Brain imaging in clinical psychiatry. Marcel Dekker, Inc., New York.

MacFall, J.R., Byrum, C.E., Parashos, I., Early, B., Charles, H.C., Chittilla, V., Boyko, O.B., Upchurch, L., Krishnan, K.R.R., 1994. Relative accuracy and reproducibility of regional MRI brain volumes for point-counting methods. Psychiatry Research: Neuroimaging 55, 167-177.

Mayhew, T.M., Olsen, D.R., 1991. Magnetic resonance imaging (MRI) and model-free estimates of brain volume determined using the Cavalieri principle. Journal of Anatomy 178, 133-144.

Nemeroff, C., Krishnan, K.R., Reed, D., Leder, R., Beam, C., Dunnick, N.R., 1992. Adrenal gland enlargement in major depression. A computed tomographic study. Archives of General Psychiatry 5, 387.

Oster, S., Christoffersen, P., Gundersen, H.J., Nielson, J.O., Pakkenberg, B., Pedersen, C., 1993. Cerebral atrophy in AIDS: a stereological study. Acta Neuropathologica 85, 617-622.

Pache, J.C., Roberts, N., Vock, P., Zimmerman, A., Cruz-Orive, L.M., 1993. Vertical LM sectioning and parallel CT scanning designs for stereology: application to human lung. Journal of Microscopy 170, 9-24.

Robb, R.A., Barillot, C., 1989. Interactive display and analysis of 3-D medical images. IEEE Transactions in Medical Imaging 8, 217-226.

Roberts, N., 1993. Unbiased estimation of volume: some notes for ANALYZE™ users. In: Mayo Biomedical Imaging Resource (Ed.), ANALYZE version 6.2 Reference Manual. Rochester, MN, pp. III-284 - III-289.

Sheline, Y.I., Black, K.J., Lin, D.Y., Christensen, G.E., Gado, M.H., Brunsden, B.S., Vannier, M.W., 1996a. Stereological MRI volumetry of the frontal lobe. Psychiatry Research: Neuroimaging 67, 203-214.

Sheline, Y.I., Black, K.J., Lin, D.Y., Pimmel, J., Wang, P., Haller, J.W., Csernansky, J.G., Gado, M.H., Walkup, R., Brunsden, B.S., Vannier, M.W., 1995. MRI volumetry of prefrontal cortex. In: Loew, M.H. (Ed.), Image Processing (SPIE Proceedings vol. 2434). pp. 766-770.

Sheline, Y.I., Wang, P.W., Gado, M.H., Csernansky, J.G., Vannier, M., 1996b. Hippocampal atrophy in recurrent major depression. Proceedings of the National Academy of Sciences of the U S A 93, 3908-3913.

**Table 1.**

| image description | # of sampling grids tested | maximum $CV_{random}$ (%) | maximum $CV_{fixed}$ (%) | median ratio $CV_{fixed}$ / $CV_{random}$ | # of grids for which $CV_{random} < CV_{fixed}$ | # of grids for which $CV_{fixed} < CV_{random}$ | $p$ (1 tail) |
|---|---|---|---|---|---|---|---|
| right cylinders (cube & circular cylinders) | 111 | 14.879 | 29.460 | 1.993 | 109 | 0 | $2 \times 10^{-33}$ |
| cube at 45° | 32 | 5.680 | 6.113 | 1.010 | 17 | 15 | 0.43 |
| human brain, axial | 204 | 7.425 | 8.482 | 1.133 | 194 | 10 | $1 \times 10^{-45}$ |
| human brain, coronal | 207 | 7.383 | 8.575 | 1.146 | 174 | 33 | $1 \times 10^{-24}$ |
| baboon brain, axial | 50 | 2.956 | 2.844 | 0.944 | 18 | 32 | 0.98 |
| baboon brain, coronal | 50 | 2.589 | 2.690 | 1.041 | 39 | 11 | $5 \times 10^{-5}$ |
| putamen, axial | 122 | 8.860 | 11.781 | 1.060 | 95 | 27 | $2 \times 10^{-10}$ |
| putamen, coronal | 186 | 8.253 | 12.841 | 1.295 | 182 | 4 | $5 \times 10^{-49}$ |
| hippocampus, axial | 195 | 7.428 | 8.650 | 1.006 | 106 | 88 | 0.10 |
| hippocampus, coronal | 193 | 7.777 | 9.040 | 0.983 | 79 | 114 | 0.995 |
| hippocampus, long axis | 196 | 7.557 | 10.758 | 1.153 | 139 | 57 | $2 \times 10^{-9}$ |

**Table 2.**

| image description | correlation of $CV_{random}$ with (# of "hits")$^{-1/2}$ ($r$) | largest deviation of $CV_{random}$ from least-squares prediction (× 100) |
|---|---|---|
| human brain, axial | 0.952 | 1.64 |
| human brain, coronal | 0.993 | 0.29 |
| baboon brain, axial | 0.889 | 0.38 |
| baboon brain, coronal | 0.939 | 0.20 |
| putamen, axial | 0.812 | 2.10 |
| putamen, coronal | 0.948 | 1.17 |
| hippocampus, axial | 0.960 | 1.55 |
| hippocampus, coronal | 0.958 | 1.88 |
| hippocampus, long axis | 0.965 | 1.54 |

**Table legends:**

Table 1.

Efficiency of 3D stereologic volumetry using either fixed-grid or random-grid placement of sampling grid across sampled sections, measured by 100,000 trials with each method. “Long axis” = sectioned approximately perpendicularly to the long axis of the hippocampus. See text for other definitions.

Table 2.

For a variety of neuroanatomical images, the number of test grid points intersecting the object of interest (“hits”) is by far the main determinant of relative variance. After accounting for the total number of hits with least-squares regression, changes in how those hits are distributed (e.g. more slices with fewer hits each) add little to the relative variance of the method, for the images and test grids examined. See Results and Discussion.

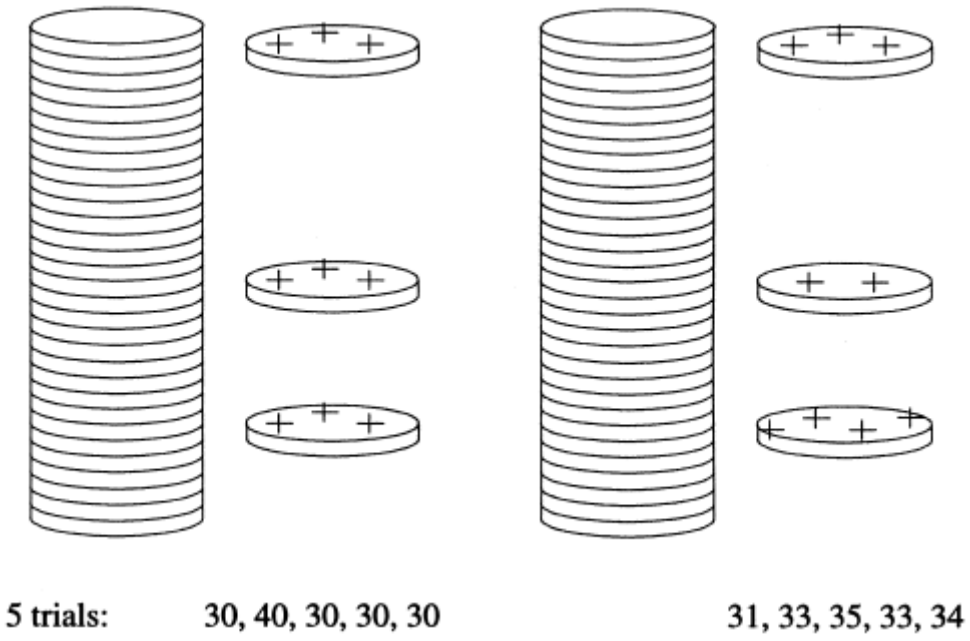


Figure 1.

This figure demonstrates the difference between the fixed-grid and random-grid approaches to implementing stereologic volumetry in 3D discrete images (see text for definitions). The drawing represents a cylindrical object whose true volume is 33, spanning several adjacent sections of a 3D image. In a typical stereologic volume measurement, 10 sections at a fixed interval might be subjected to an area measurement using test points in a square lattice; three such sections are shown here. On the *left* is the fixed-grid case. Although the sampling grid placement is random on the first section, it is maintained in a fixed position across all subsequent slices. The grid placement shown here would lead to a volume estimate of 30. Below the object is one possible sequence of repeated volume measurements using the fixed-grid method; note that a volume estimate of 33 is not possible. The figure on the *right* represents the random-grid method. Here volume is measured using the same slices and the same initial grid position as in the fixed-grid

method, but the results in general fall closer to the true measurement (*i.e.* variance is less). This is intuitive since each random-grid result is essentially equivalent to averaging ten fixed-grid trials. For a proof, see Results.

## Figure 2

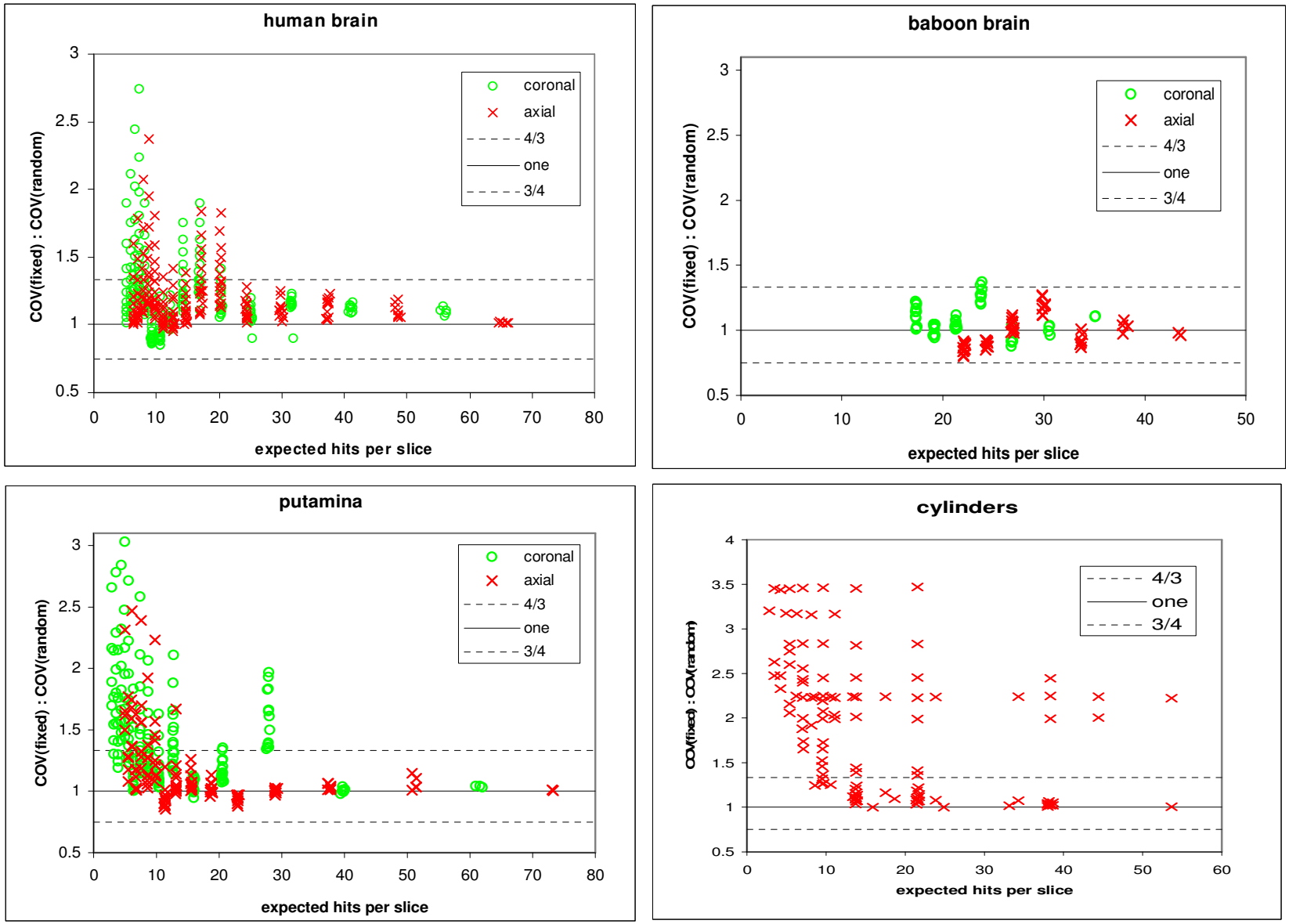
human brain
COV(fixed) : COV(random)
expected hits per slice
coronal
axial
4/3
one
3/4
baboon brain
COV(fixed) : COV(random)
expected hits per slice
coronal
axial
4/3
one
3/4
putamina
COV(fixed) : COV(random)
expected hits per slice
coronal
axial
4/3
one
3/4
cylinders
expected hits per slice
4/3
one
3/4

Figure 2.

As shown here for several different objects, the extent to which the random-grid method has lower variance than the fixed-grid method is a function of the average number of "hits" (intersections of test grid with object) on each "slice" (nonempty cross-section). When the average number of hits per slice (horizontal axis) exceeds 10-20, the relative variance of the two methods becomes similar, shown here as their ratio (vertical axis) approaching unity. However, for fewer hits per slice, the variance of the fixed-grid method can be substantially higher than that of the random-grid method.

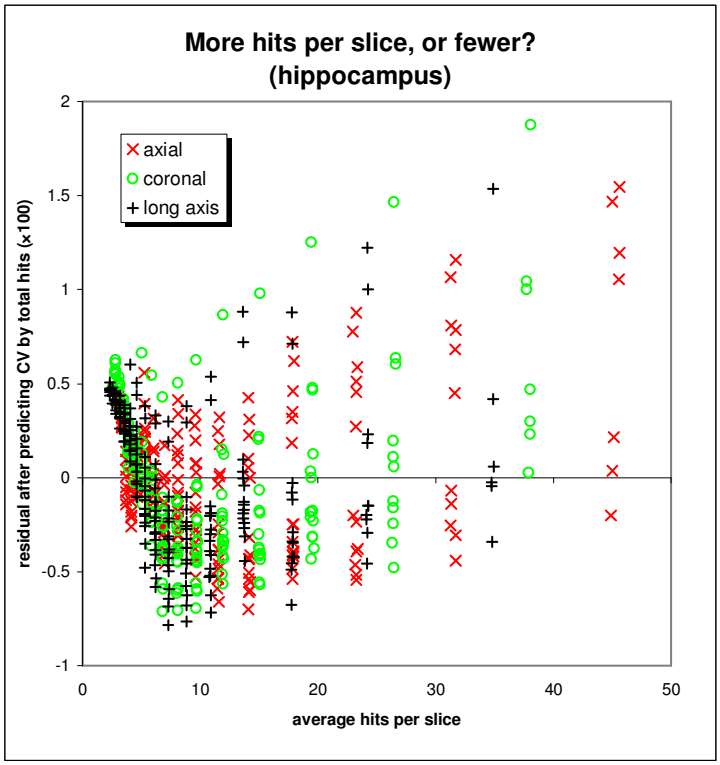
More hits per slice, or fewer?
(hippocampus)
axial
coronal
long axis
residual after predicting CV by total hits (×100)
average hits per slice
2
1.5
1
0.5
0
-0.5
-1
0
10
20
30
40
50

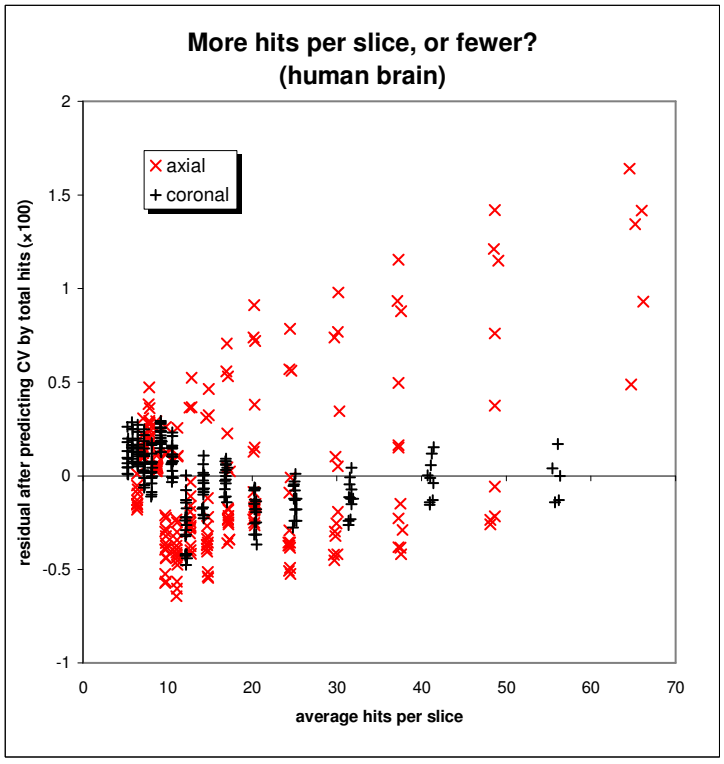
More hits per slice, or fewer?
(human brain)
axial
coronal
residual after predicting CV by total hits (×100)
average hits per slice
2
1.5
1
0.5
0
-0.5
-1
0
10
20
30
40
50
60
70

Fig. 3.

Figure 3.

After removing the effect of total number of test points intersecting the object ("hits"), relative variance of stereologic volumetry *when implemented using the random-grid method* is not greatly affected by the distribution of hits across slices within the range examined. See Materials and Methods, last paragraph, and Results.